第 29 卷第 11 期 中国有色金属学报 2019 年 11 月
Volume 29 Number 11 The Chinese Journal of Nonferrous Metals November 2019
DOI：10.19476/j.ysxb.1004.0609.2019.11.17

Al 基五元高熵合金的热力学研究

张 雷[1,3]，陈红梅[2]，陶小马[2]，欧阳义芳[2]

(1. 广西教育学院 数学与信息科学学院，南宁 530023；
2. 广西大学 物理科学与工程技术学院，南宁 530004；
3. 广西教育学院 智能计算及模拟研究所，南宁 530023)

摘 要：高熵合金具有高硬度、高强度、良好的耐磨性以及耐腐蚀性等优异性能。高熵合金一般由 5 种或 5 种以上金属元素组成，不同金属元素可以提高合金内部混乱程度，形成具有简单晶格结构的固溶体相。Miedema 理论和几何扩展模型可以计算多组元合金固溶状态的混合焓，而混合焓对高熵合金的固溶相的形成有重要影响。本文利用扩展 Miedema 理论计算 $Al_x(CuMgSi\text{-}T)_{1-x}$ (T=Ag, As, Au, B, Ba, Be, Bi, C, Ca, Cd, Co, Cr, Cs, Fe, Ga, Ge, Hf, Hg, In, Ir, K, La, Li, Mn, Mo, N, Na, Nb, Ni, Os, P, Pb, Pd, Pt, Rb, Re, Rh, Ru, Sb, Sc, Sn, Sr, Ta, Tc, Ti, Tl, V, W, Y, Zn, Zr) 五元合金体系固溶状态的混合焓，用已有高熵合金混合焓和原子尺寸判据来预测了 $Al_x(CuMgSi\text{-}T)_{1-x}$ 五元高熵合金的成分范围。计算结果表明，$Al_x(CuMgSi\text{-}T)_{1-x}$(T=Ag, As, Au, Cd, Co, Cr, Fe, Ga, Ge, Hf, Hg, In, Ir, Li, Mn, Mo, Nb, Ni, Os, Pd, Pt, Re, Rh, Ru, Sb, Sc, Sn, Ta, Tc, Ti, V, W, Zn, Zr)五元体系合金混合焓和原子尺寸方均差 δ 参数满足相关判据，易于形成五元高熵合金。采用混合焓和 δ 参数判据可以预测高熵合金的成分，为高熵合金设计提供较为精确的热力学数据。

关键词：Miedema 理论；几何模型；高熵合金；混合焓；原子尺寸；方均差
文章编号：1004-0609(2019)-11-2601-08 **中图分类号**：TG 146.2 **文献标志码**：A

传统合金在元素组成上大多以 1~2 种元素作为主要元素，通过添加少量其他元素来获得所需要的性能，添加元素种类过多会增加产生脆性金属间化合物的可能性，进而导致合金脆性增加; 元素种类少又不利于合金性能的改善，因此合金元素种类及比例选取与合金性能的优劣关系一直是材料研究的主要内容之一。近 10 年来，高熵合金(HEAs)以其优异性能成为新型金属材料领域中的研究热点[1−9]。高熵合金一般由 5 种或 5 种以上金属元素组成，不同金属元素可以提高合金内部排列的混乱程度，形成具有简单晶格结构且热稳定性高的固溶相。高熵合金具有高硬度、高强度、良好的耐磨性以及耐腐蚀性等传统合金所不能同时具备的优异性能。

铝合金具有密度低、延展性好、成本低等优点，在各领域都得到了广泛应用。铝合金只有钢密度的三分之一，比强度高，具有很大的减重潜力。在保证材料强度和安全的情况下可以减重 50%以上，在汽车工业、航空航天、船舶等领域有重要应用[10−12]。BUTLER 等[13−15]和 WANG 等[16]研究了含 Al 的多组元合金，认为 Al 元素能够改善合金的抗氧化性能；王浩玉等[17]提出 Al 元素能够显著降低 $Al_xCrFeNiTi$ 高熵合金的混合焓，进而提高其合金形成能力，适量的 Al 元素对多组元合金的形成和相关性能是有利的。Al-Cu-Mg-Si 体系合金具有良好的流动性和浇注性，适合用于制造发动机室。Al-Cu-Mg-Si 体系中的多种合金发现存在平衡 Q 相，该相可以增加铝基体强度[18−20]。WOLVERTON[21]和 RAVI 等[22]研究了 Al-Cu-Mg-Si 的晶体结构；用第一性原理[21−24]、CALPHAD[25−28]等方法研究 Al-Cu-Mg-Si 体系相关相的稳定性也有相关报道。

高熵合金设计已有相关理论方法[29−30]和实验制备方法[4, 6−7, 31]，其设计关键在于通过组成元素按一定比例相互溶合，形成 FCC、BCC 或 HCP 的简单固溶体，且要尽量避免金属间化合物或其他非金属夹杂物

基金项目：国家自然科学基金资助项目(51531009，11464001)；广西自然科学基金资助项目(2016GXNSFBA380166)；广西高校中青年教师基础能力提升项目(2017KY1472)
收稿日期：2018-12-02；**修订日期**：2019-04-02
通信作者：欧阳义芳，教授，博士；电话：0771-3237386；E-mail：ouyangyf@gxu.edu.cn

的形成。张勇等[32−34]指出高熵合金的混合焓范围在−15~5 kJ/mol，还总结归纳出 Ω、δ 等参数，指出多组元合金中以 $\Omega\geqslant 1.1$、$\delta\leqslant 6.6\%$作为形成固溶相的经验判据。

相的稳定性与吉布斯自由能有密切关系，当选定合金组元数后，体系的混合焓及原子尺寸差异对自由能的影响较大，综合考虑合金固溶状态的混合焓及组元间原子尺寸差对于设计高熵合金有重要意义。近年来 Miedema 理论得到了不断完善[35−37]，与几何扩展模型相结合可以较好地预测多元合金热力学性质[38−42]。本文结合 Miedema 和几何扩展模型计算 Al_x(CuMgSi-T)$_{1-x}$ (T=Ag, As, Au, B, Ba, Be, Bi, C, Ca, Cd, Co, Cr, Cs, Fe, Ga, Ge, Hf, Hg, In, Ir, K, La, Li, Mn, Mo, N, Na, Nb, Ni, Os, P, Pb, Pd, Pt, Rb, Re, Rh, Ru, Sb, Sc, Sn, Sr, Ta, Tc, Ti, Tl, V, W, Y, Zn, Zr)五元合金的混合焓，同时考虑原子尺寸差异，从热力学角度计算预测五元高熵合金形成的可能性。

1 计算方法

1.1 多元合金的混合焓

ZHANG 等[35−36]和 SUN 等[37]对 Miedema 理论在计算二元过渡族的形成焓误差作了修正。对于多元合金系统，几何扩展模型充分考虑了组元间的相互作用，OUYANG 等[39−41]将 Miedema 理论结合几何扩展模型较好地预测多元合金的热力学性质。利用 Ouyang 模型可以得到五元合金的混合焓，具体可表示为：

$$\begin{aligned}\Delta H_{\mathrm{mix}}=&\frac{x_1x_2}{y_{12}^1y_{12}^2}\Delta H_{12}(y_{12}^1,y_{12}^2)+\frac{x_1x_3}{y_{13}^1y_{13}^3}\Delta H_{13}(y_{13}^1,y_{13}^3)+\\&\frac{x_1x_4}{y_{14}^1y_{14}^4}\Delta H_{14}(y_{14}^1,y_{14}^4)+\frac{x_1x_5}{y_{15}^1y_{15}^5}\Delta H_{15}(y_{15}^1,y_{15}^5)+\\&\frac{x_2x_3}{y_{23}^2y_{23}^3}\Delta H_{23}(y_{23}^2,y_{23}^3)+\frac{x_2x_4}{y_{24}^2y_{24}^4}\Delta H_{24}(y_{24}^2,y_{24}^4)+\\&\frac{x_2x_5}{y_{25}^2y_{25}^5}\Delta H_{25}(y_{25}^2,y_{25}^5)+\frac{x_3x_4}{y_{34}^3y_{34}^4}\Delta H_{34}(y_{34}^3,y_{34}^4)+\\&\frac{x_3x_5}{y_{35}^3y_{35}^5}\Delta H_{35}(y_{35}^3,y_{35}^5)+\frac{x_4x_5}{y_{45}^4y_{45}^5}\Delta H_{45}(y_{45}^4,y_{45}^5)\end{aligned}\tag{1}$$

式中：ΔH_{mix} 为五元合金的混合焓，ΔH_{ij} $(i,j=1,2,3,4,5)$是相应二元系统的混合焓，x_i 是系统中组分的摩尔分数，y_{ij}^i 和 y_{ij}^j 是五元系统外推到相应的二元系统中对应组分 i 和 j 的摩尔分数，由下列这组公式表示：

$$\begin{cases}y_{12}^1=x_1+\delta_{12}^1(x_3+x_4+x_5)\quad y_{12}^2=x_2+\delta_{12}^2(x_3+x_4+x_5)\\y_{13}^1=x_1+\delta_{13}^1(x_2+x_4+x_5)\quad y_{13}^3=x_3+\delta_{13}^2(x_2+x_4+x_5)\\y_{14}^1=x_1+\delta_{14}^1(x_2+x_3+x_5)\quad y_{14}^4=x_4+\delta_{14}^4(x_2+x_3+x_5)\\y_{15}^1=x_1+\delta_{15}^1(x_2+x_3+x_4)\quad y_{15}^5=x_5+\delta_{15}^5(x_2+x_3+x_4)\\y_{23}^2=x_2+\delta_{23}^2(x_1+x_4+x_5)\quad y_{23}^3=x_3+\delta_{23}^3(x_1+x_4+x_5)\\y_{24}^2=x_2+\delta_{24}^2(x_1+x_3+x_5)\quad y_{24}^4=x_4+\delta_{24}^4(x_1+x_3+x_5)\\y_{25}^2=x_2+\delta_{25}^2(x_1+x_3+x_4)\quad y_{25}^5=x_5+\delta_{25}^5(x_1+x_3+x_4)\\y_{34}^3=x_3+\delta_{34}^3(x_1+x_2+x_5)\quad y_{34}^4=x_4+\delta_{34}^4(x_1+x_2+x_5)\\y_{35}^3=x_3+\delta_{35}^3(x_1+x_2+x_4)\quad y_{35}^5=x_5+\delta_{35}^5(x_1+x_2+x_4)\\y_{45}^4=x_4+\delta_{45}^4(x_1+x_2+x_3)\quad y_{45}^5=x_5+\delta_{45}^5(x_1+x_2+x_3)\end{cases}\tag{2}$$

$$\begin{cases}\delta_{12}^1=\lambda_1/(\lambda_1+\lambda_2),\delta_{12}^2=\lambda_2/(\lambda_1+\lambda_2)\\\delta_{13}^1=\lambda_1/(\lambda_1+\lambda_3),\delta_{13}^3=\lambda_3/(\lambda_1+\lambda_3)\\\delta_{14}^1=\lambda_1/(\lambda_1+\lambda_4),\delta_{14}^4=\lambda_4/(\lambda_1+\lambda_4)\\\delta_{15}^1=\lambda_1/(\lambda_1+\lambda_5),\delta_{15}^5=\lambda_5/(\lambda_1+\lambda_5)\\\delta_{23}^2=\lambda_2/(\lambda_2+\lambda_3),\delta_{23}^3=\lambda_3/(\lambda_2+\lambda_3)\\\delta_{24}^2=\lambda_2/(\lambda_2+\lambda_4),\delta_{24}^4=\lambda_4/(\lambda_2+\lambda_4)\\\delta_{25}^2=\lambda_2/(\lambda_2+\lambda_5),\delta_{25}^5=\lambda_5/(\lambda_2+\lambda_5)\\\delta_{34}^3=\lambda_3/(\lambda_3+\lambda_4),\delta_{34}^4=\lambda_4/(\lambda_3+\lambda_4)\\\delta_{35}^3=\lambda_3/(\lambda_3+\lambda_5),\delta_{35}^5=\lambda_5/(\lambda_3+\lambda_5)\\\delta_{45}^4=\lambda_4/(\lambda_4+\lambda_5),\delta_{45}^5=\lambda_5/(\lambda_4+\lambda_5)\end{cases}\tag{3}$$

$$\begin{cases}\lambda_1=(\Delta H_{21}-\Delta H_{31})^2+(\Delta H_{21}-\Delta H_{41})^2+\\\qquad(\Delta H_{21}-\Delta H_{51})^2+(\Delta H_{31}-\Delta H_{41})^2+\\\qquad(\Delta H_{31}-\Delta H_{51})^2+(\Delta H_{41}-\Delta H_{51})^2\\\lambda_2=(\Delta H_{12}-\Delta H_{32})^2+(\Delta H_{12}-\Delta H_{42})^2+\\\qquad(\Delta H_{12}-\Delta H_{52})^2+(\Delta H_{32}-\Delta H_{42})^2+\\\qquad(\Delta H_{32}-\Delta H_{52})^2+(\Delta H_{42}-\Delta H_{52})^2\\\lambda_3=(\Delta H_{13}-\Delta H_{23})^2+(\Delta H_{13}-\Delta H_{43})^2+\\\qquad(\Delta H_{13}-\Delta H_{53})^2+(\Delta H_{23}-\Delta H_{43})^2+\\\qquad(\Delta H_{23}-\Delta H_{53})^2+(\Delta H_{43}-\Delta H_{53})^2\\\lambda_4=(\Delta H_{14}-\Delta H_{24})^2+(\Delta H_{14}-\Delta H_{34})^2+\\\qquad(\Delta H_{14}-\Delta H_{54})^2+(\Delta H_{24}-\Delta H_{34})^2+\\\qquad(\Delta H_{24}-\Delta H_{54})^2+(\Delta H_{34}-\Delta H_{54})^2\\\lambda_5=(\Delta H_{15}-\Delta H_{25})^2+(\Delta H_{15}-\Delta H_{35})^2+\\\qquad(\Delta H_{15}-\Delta H_{45})^2+(\Delta H_{25}-\Delta H_{35})^2+\\\qquad(\Delta H_{25}-\Delta H_{45})^2+(\Delta H_{35}-\Delta H_{45})^2\end{cases}\tag{4}$$

二元合金系统的混合焓 ΔH_{ij} 的计算及相关计算参数可由文献[43]得到。

1.2　δ 参数

δ 参数表示组成合金的全部元素的原子尺寸均方差，表示如下

$$\delta=\sqrt{\sum_{i=1}^{n}x_i\left(1-\frac{r_i}{\bar{r}}\right)^2} \tag{5}$$

$$\bar{r}=\sum_{i=1}^{n}x_i r_i \tag{6}$$

式中：x_i 为系统中组分的摩尔分数；r_i 为对应组成元素的原子半径，r_i 取自文献[44]；$\bar{r}$ 为所有组分的原子半径加权值。

2　计算结果及讨论

2.1　Al-Cu-Mg-Si 四元体系合金

Al-Cu-Mg-Si 四元体系中的 Q 相不仅是一个显著的增强相，而且是一个含有多重化学计量比的化合物，如 $Al_5Cu_2Mg_8Si_6$[45−46]、$Al_4Cu_1Mg_5Si_4$[47]、$Al_4Cu_2Mg_8Si_7$[48]、$Al_{17}Cu_9Mg_{45}Si_{29}$[27]和 $Al_{3.5}Cu_2Mg_{9.5}Si_6$[27]等。用 Ouyang 扩展 Miedema 模型计算了文献报道的所有化合物的形成焓，并与第一性原理计算、相图计算得到的理论值[21−24, 26−28]进行了比较，如表 1 所示。

由表 1 可以看出，CALPHD 计算和第一性原理计算得到的结果比较接近，扩展 Miedema 模型计算的焓值绝对值相比前两种方法的计算值绝对值偏小，但趋势一致，整体上合理吻合。WOLVERTON[21]用第一原理计算了 Q 相 $Al_xCu_2Mg_{12-x}Si_7$ 形成焓，$Al_3Cu_2Mg_9Si_7$ 在 Al 原子的四个不同占位下，形成焓为−17.6~−7.0 kJ/mol，$Al_4Cu_2Mg_8Si_7$ 在 Al 原子的四个不同占位下，形成焓为−15.6~−12.4 kJ/mol，因此 Al 原子占位会引起 Q 相形成焓的变化。而 Miedema 模型计算时没有考虑到晶体结构对形成焓的影响，因此产生偏差。由于 Al-Cu-Mg-Si 四元体系中的化合物的形成焓无实验结果，目前不能进一步比较。

2.2　$Al_x(CuMgSi\text{-}T)_{1-x}$ 五元体系合金

将元素 T (T=Ag, As, Au, B, Ba, Be, Bi, C, Ca, Cd, Co, Cr, Cs, Fe, Ga, Ge, Hf, Hg, In, Ir, K, La, Li, Mn, Mo, N, Na, Nb, Ni, Os, P, Pb, Pd, Pt, Rb, Re, Rh, Ru, Sb, Sc, Sn, Sr, Ta, Tc, Ti, Tl, V, W, Y, Zn, Zr) 加入 Al-Cu-Mg-Si 四元体系，考虑 Al 元素成分变化对五元高熵合金混合焓的影响，计算了 $Al_x(CuMgSi\text{-}T)_{1-x}$ (x=0.3~0.7) 五元合金体系的固溶态混合焓。不同 T 元素的五元合金混合焓与 δ 参数如图 1 所示。

表 1　Al-Cu-Mg-Si 四元合金的形成焓

Table 1　Formation enthalpies for Al-Cu-Mg-Si quaternary compounds

Compound	Formation enthalpy/(kJ·mol^{-1})		
	CALPHAD	First-principles	Present work
$AlCu_2Mg_{11}Si_7$		−15.5[21]	−7.14
		−13.1[24]	
$Al_2Cu_2Mg_{10}Si_7$		−16.8[21]	−7.50
		−14.6[24]	
$Al_3Cu_2Mg_9Si_7$	−17.9[26]	−17.6[21]	−7.68
	−17.4[28]	−16.1[22]	
		−17.4[22]	
		−14.9[23]	
		−15.7[24]	
		−17.6[28]	
$Al_4Cu_2Mg_8Si_7$		−15.7[21]	−7.65
		−14.2[22]	
		−15.5[22]	
		−13.7[24]	
$Al_5Cu_2Mg_7Si_7$		−13.0[21]	−7.41
$Al_5Cu_2Mg_8Si_6$	−35.5[28]	−12.0[22]	−7.07
		−12.9[22]	
		−11.9[24]	
		−12.5[28]	
$Al_4Cu_1Mg_5Si_4$			−6.06
$Al_{17}Cu_9Mg_{45}Si_{29}$	−18.0[27]		−6.96
$Al_{3.5}Cu_2Mg_{9.5}Si_6$		−11.4[27]	−7.07

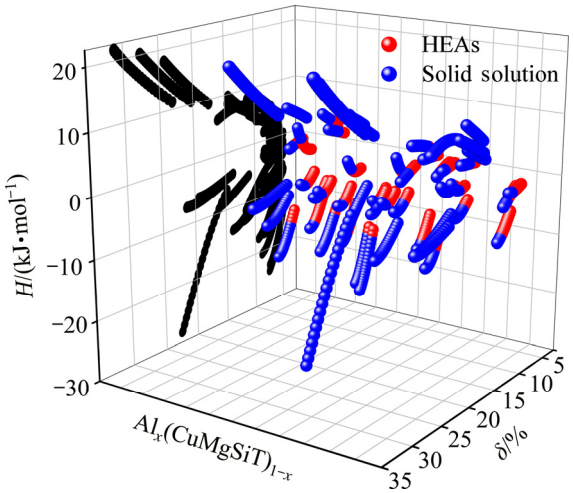

图 1　$Al_x(CuMgSi\text{-}T)_{1-x}$ 体系合金混合焓与 δ 参数(黑色圆点表示合金混合焓与 δ 参数的关系；红色球体表示高熵合金的成分；蓝色球体表示合金固溶状态的成分)

Fig. 1　Mixing enthalpies and parameter δ for $Al_x(CuMgSi\text{-}T)_{1-x}$ quinary system alloys (black dot indicates relationship between mixing enthalpies and parameter δ; red ball indicates composition point for HEA; blue ball indicates composition point for solid solution status)

从图1中可以看出，$Al_x(CuMgSi\text{-}T)_{1-x}$体系中符合判据$-15\ kJ/mol<\Delta H_{mix}<5\ kJ/mol$，且$\delta<6.6\%$的成分主要集中在原子尺寸均方差10%以内，少部分合金原子尺寸均方差很大。这些原子尺寸差异较大的合金分两类，一类是掺入了B、C、N、P、Be等原子尺寸较小的非金属和碱土金属，另一类是掺入了Na、K、Rb、Cs、Ca、Sr、Ba、Y、La等原子尺寸较大的碱金属、碱土金属等元素。这两类元素的掺入与成分变化同时作用，导致原子尺寸方均差变得较大。从图1还可看出，某些体系合金的焓值中表现出部分符合判据，究其原因，主要是Al元素成分的变化引起同体系的原子尺寸均方差的变化。

图1中符合判据的成分点非常密集，为了进一步分析合金混合焓、元素成分及δ参数之间的关系，图2给出了$Al_x(CuMgSi\text{-}T)_{1-x}$五元合金体系中符合判据的所有合金体系，其中T=Ag, As, Au, Cd, Co, Cr, Fe,

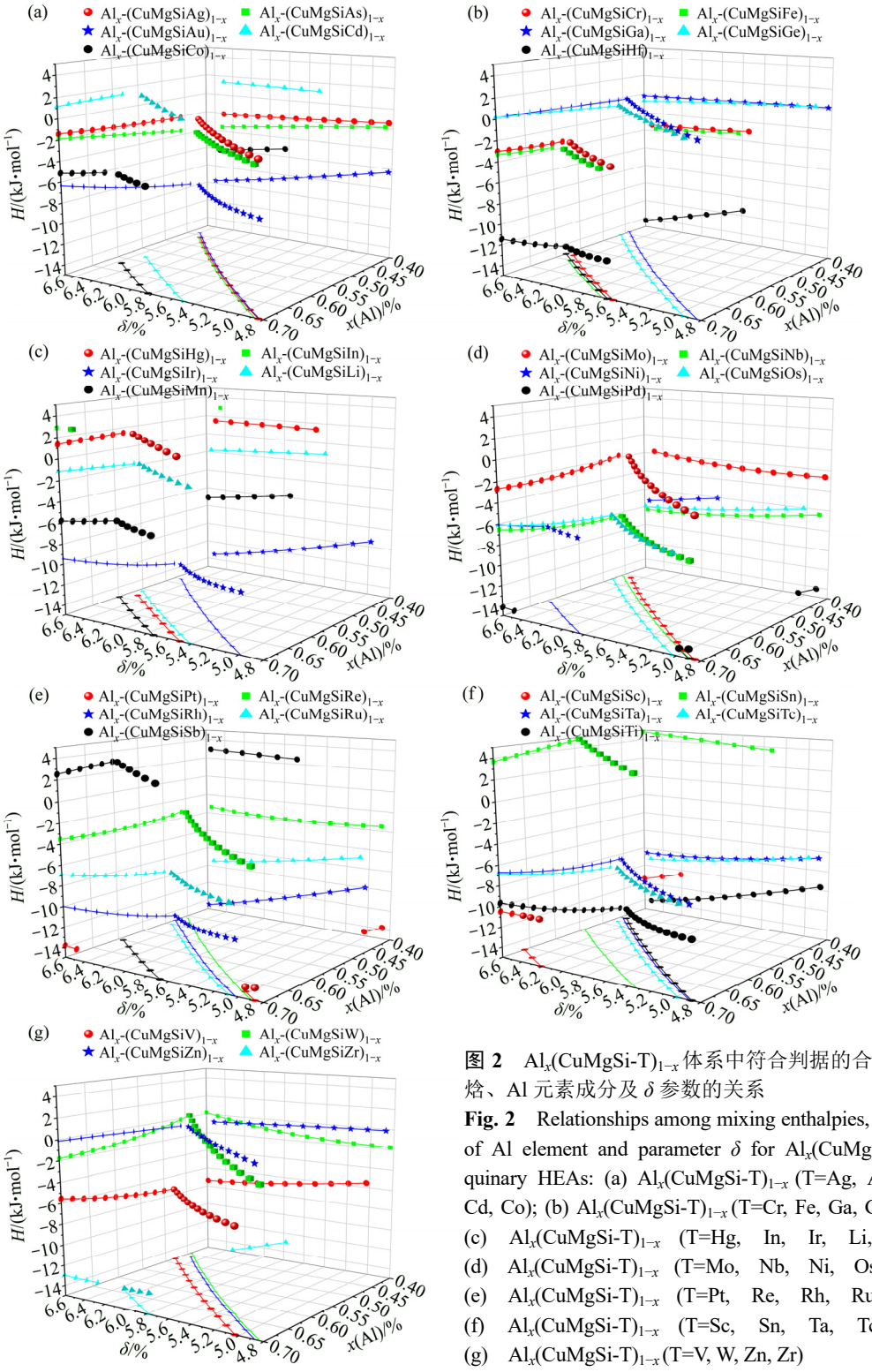

图2 $Al_x(CuMgSi\text{-}T)_{1-x}$体系中符合判据的合金混合焓、Al元素成分及$\delta$参数的关系

Fig. 2 Relationships among mixing enthalpies, content of Al element and parameter δ for $Al_x(CuMgSi\text{-}T)_{1-x}$ quinary HEAs: (a) $Al_x(CuMgSi\text{-}T)_{1-x}$ (T=Ag, As, Au, Cd, Co); (b) $Al_x(CuMgSi\text{-}T)_{1-x}$ (T=Cr, Fe, Ga, Ge, Hf); (c) $Al_x(CuMgSi\text{-}T)_{1-x}$ (T=Hg, In, Ir, Li, Mn); (d) $Al_x(CuMgSi\text{-}T)_{1-x}$ (T=Mo, Nb, Ni, Os, Pd); (e) $Al_x(CuMgSi\text{-}T)_{1-x}$ (T=Pt, Re, Rh, Ru, Sb); (f) $Al_x(CuMgSi\text{-}T)_{1-x}$ (T=Sc, Sn, Ta, Tc, Ti); (g) $Al_x(CuMgSi\text{-}T)_{1-x}$ (T=V, W, Zn, Zr)

Ga, Ge, Hf, Hg, In, Ir, Li, Mn, Mo, Nb, Ni, Os, Pd, Pt, Re, Rh, Ru, Sb, Sc, Sn, Ta, Tc, Ti, V, W, Zn, Zr。

从图 2 中可以看出，大部分体系都呈现出相对一致的变化趋势，具体如下：

1) x_{Al}-δ 投影面上全部呈现出单调趋势，δ 参数随着 Al 含量的增加逐渐减小，当 Al 元素占比较小时，合金中其他元素对于原子尺寸差异的贡献较大，进而影响到原子尺寸均方差。

2) 对于 $Al_x(CuMgSi\text{-}T)_{1-x}$ (T=Ag, As, Au, Co, Cr, Fe, Ga, Ge, Hf, Ir, Li, Mn, Nb, Ni, Os, Pd, Pt, Rh, Ru, Sc, Ta, Tc, Ti, V, Zn, Zr)体系，x_{Al}-H 和 δ-H 投影面呈现出明显的单调变化趋势，混合焓随 Al 元素含量的增加而增大、随 δ 参数变小而逐渐增大；对于 $Al_x(CuMgSi\text{-}T)_{1-x}$ (T=Mo, Sb, Sn, W)体系，呈现出相反的单调变化趋势，混合焓随 Al 元素含量的增加而减小、随 δ 参数减小而逐渐减小；对于 $Al_x(CuMgSiCd)_{1-x}$ 和 $Al_x(CuMgSiHg)_{1-x}$ 体系，在 x_{Al}-H 和 δ-H 投影面混合焓均没有明显的变化；对于 $Al_x(CuMgSiRe)_{1-x}$ 体系，在 x_{Al}-H 投影面混合焓随 Al 元素含量的增加先减小后增大，而 δ-H 投影面混合焓随 δ 参数减小先减小后增大。

合金混合焓主要由元素种类及成分决定，而形成焓对合金的稳定性有重要意义。在合金化过程中，一般趋向于形成诸多相中能量最低的相。MIEDEMA 等[49]对二元合金系统的研究表明混合焓可以显著的影响合金相的形成，更负的混合焓会利于金属间化合物的形成。与此类似，对于多元合金体系而言，其合金化过程更加复杂，混合焓越负，合金组元间的键合力越强，越容易形成更加稳定的金属间化合物，反之，混合焓越正，组元间的混合能力越差，组元间不容易结合倾向于分离。因此，高熵合金的混合焓必须在合适的范围，使之形成能够保留液态混乱程度的固溶相。由此可见，图 2 中 $Al_x(CuMgSiRe)_{1-x}$ 中一部分合金体系受到 Al 元素的含量变化的影响，进而导致过大或是过小的混合焓，不利于高熵合金中固溶相的形成。

TAKEUCHI 等[50]在非晶设计中指出合金组成元素的原子尺寸差异对非晶的形成产生贡献。在高熵合金设计中也存在类似情况，大多数高熵合金中的元素组分接近，原子排列在原来的晶格位置上，当有原子尺寸差异特别大的原子时，原有状态将会被破坏，不利于固溶状态的形成；此外，过大的原子尺寸差异会导致过大的晶格畸变，产生相应的应变能，而应变能为正，会导致合金混合焓向正偏移，不利于形成稳定的固溶相。从图 2 中可以看出，合金的元素组成和成分都会影响到合金的原子尺寸均方差。

3　结论

1) 利用 Miedema 理论和几何扩展模型计算了 Al-Cu-Mg-Si 四元合金体系中文献报道的所有化合物形成焓，计算值与 CALPHAD 计算和第一性原理计算的理论值合理吻合。

2) 计算了 $Al_x(CuMgSi\text{-}T)_{1-x}$ (T=Ag, As, Au, B, Ba, Be, Bi, C, Ca, Cd, Co, Cr, Cs, Fe, Ga, Ge, Hf, Hg, In, Ir, K, La, Li, Mn, Mo, N, Na, Nb, Ni, Os, P, Pb, Pd, Pt, Rb, Re, Rh, Ru, Sb, Sc, Sn, Sr, Ta, Tc, Ti, Tl, V, W, Y, Zn, Zr)五元合金体系的固溶态混合焓，依据 $-15\ kJ/mol < \Delta H_{mix} < 5\ kJ/mol$ 和 $\delta < 6.6\%$ 判据预测了 $Al_x(CuMgSi\text{-}T)_{1-x}$ 体系合金形成高熵合金的成分范围；体系中多数合金的混合焓随 Al 含量的增加而增大、随 δ 参数减小而逐渐减小；少部分合金混合焓随 Al 含量的增加而减小、随 δ 参数减小而逐渐减小。

3) $Al_x(CuMgSi\text{-}T)_{1-x}$ 五元合金体系中部分成分能够形成高熵合金，其中 $Al_x(CuMgSi\text{-}T)_{1-x}$ (T=In, Pd, Pt, Sc, Zr)五元合金体系中只能少部分形成高 Al 含量的高熵合金；$Al_x(CuMgSi\text{-}T)_{1-x}$ (T=B, Ba, Be, Bi, C, Ca, Cs, K, La, N, Na, P, Pb, Rb, Sr, Tl, Y)五元合金体系则均不能形成高熵合金。

4) 通过以混合焓和原子尺寸方均差 δ 参数为主的判据对高熵合金进行成分范围预测既简便又快捷，为高熵合金成分设计提供了可能的途径。

REFERENCES

[1] GAO M C, YEH J W, LIAW P K, ZHANG Y. High-entropy alloys: Fundamentals and applications[M]. Zurich: Springer International Publishing, 2016.

[2] ZHANG W, LIAW P K, ZHANG Y. Science and technology in high-entropy alloys[J]. Science China Materials, 2018, 61(1): 2−22.

[3] GUO N N, WANG L, LUO L S, LI X Z, CHEN R R, SU Y Q, GUO J J, FU H Z. Hot deformation characteristics and dynamic recrystallization of the MoNbHfZrTi refractory high-entropy alloy[J]. Materials Science & Engineering A, 2016, 651(3): 698−707.

[4] ZHOU S C, ZHANG P, XUE Y F, WANG F C, WANG L, CAO T Q, TAN Z, CHENG B Y, WANG B P. Microstructure evolution of $Al_{0.6}CoCrFeNi$ high entropy alloy powder prepared by high pressure gas atomization[J].

Transactions of Nonferrous Metals Society of China, 2018, 28(5): 939−945.

[5] POULIA A, GEORGATIS E, LEKATOU A, KARANTZALIS A E. Microstructure and wear behavior of a refractory high entropy alloy[J]. International Journal of Refractory Metals & Hard Materials, 2016, 57: 50−63.

[6] CHENG H, XIE Y C, TANG Q H, RAO C, DAI P Q. Microstructure and mechanical properties of FeCoCrNiMn high-entropy alloy produced by mechanical alloying and vacuum hot pressing sintering[J]. Transactions of Nonferrous Metals Society of China, 2018, 28(7): 1360−1367.

[7] 蒋 烨, 陈 可, 王 伟. 机械合金化法制备AlCoNiFeCr高熵合金涂层[J]. 中国有色金属学报, 2018, 28(9): 1784−1790.
JIANG Ye, CHEN Ke, WANG Wei. Preparation of AlCoNiFeCr high entropy alloy coating by mechanical alloying[J]. The Chinese Journal of Nonferrous Metals, 2018, 28(9): 1784-1790.

[8] 李美艳, 张 琪, 韩 彬, 王稼林. 多主元高熵合金组织性能及塑性变形的研究进展[J]. 材料热处理学报, 2019, 40(1): 1−8.
LI Mei-yan, ZHANG Qi, HAN Bin, WANG Jia-lin. Research progress on microstructure, properties and plastic deformation of high entropy alloy with multi-principal elements[J]. Transactions of Materials and Heat Treatment, 2019, 40(1): 1−8.

[9] 侯丽丽, 要玉宏, 梁霄羽, 陈 建, 刘江南. $Al_xFeCoNiB_{0.1}$高熵合金的微观组织和力学性能[J]. 稀有金属材料与工程, 2019, 48(1): 111−115.
HOU Li-li, YAO Yu-hong, LIANG Xiao-yu, CHEN Jian, LIU Jiang-nan. Microstructure and mechanical properties of $Al_xFeCoNiB_{0.1}$ high entropy alloy[J]. Rare Metal Materials and Engineering, 2019, 48(1): 111−115.

[10] AMBROZIAK A, KORZENIOWSKI M. Using resistance spot welding for joining aluminium elements in automotive industry[J]. Archives of Civil & Mechanical Engineering, 2010, 10(1): 5−13.

[11] KARIMI M R, SEDIGHI M, AFSHARI D. Thermal contact conductance effect in modeling of resistance spot welding process of aluminum alloy 6061-T6[J]. International Journal of Advanced Manufacturing Technology, 2015, 77(5/8): 85−895.

[12] FENG Y, LUO Z, LI Y, LING Z. A novel method for resistance plug welding of 7075 aluminum alloy[J]. Advanced Manufacturing Processes, 2016, 31(16): 2077−2083.

[13] BUTLER T M, WEAVER M L. Influence of annealing on the microstructures and oxidation behaviors of $Al_8(CoCrFeNi)_{92}$, $Al_{15}(CoCrFeNi)_{85}$, and $Al_{30}(CoCrFeNi)_{70}$ high-entropy alloys[J]. Metals, 2016, 6: 222.

[14] BUTLER T M, WEAVER M L. Oxidation behavior of arc melted AlCoCrFeNi multi-component high-entropy alloys[J]. Journal of Alloys and Compounds, 2016, 674: 229−244.

[15] BUTLER T M, ALFANO J P, MARTENS R L, WEAVER M L. High-temperature oxidation behavior of Al-Co-Cr-Ni-(Fe or Si) multicomponent high-entropy alloys[J]. The Journal of the Minerals, Metals & Materials Society, 2015, 16(1): 246−259.

[16] WANG S, CHEN Z, ZHANG P, CHEN C L, SHEN B L. Influence of Al content on high temperature oxidation behavior of $Al_xCoCrFeNiTi_{0.5}$ high entropy alloys[J]. Vacuum, 2019, 163: 263−268.

[17] 王浩玉, 农智升, 王继杰, 朱景川. $Al_xCrFeNiTi$系高熵合金成分和弹性性质关系[J]. 物理学报, 2019, 68(3): 212−221.
WANG Hao-yu, NONG Zhi-sheng, WANG Ji-jie, ZHU Jing-chuan. Relationship between compositions and elastic properties of $Al_xCrFeNiTi$ high entropy alloys[J]. Acta Physica Sinica, 2019, 68(3): 212−221.

[18] STARINK M J, ABEELS V M F, VAN MOURIK P. MOURIK. Lattice parameter and hardness variations resulting from precipitation and misfit accommodation in a particle-reinforced Al-Si-Cu-Mg alloy[J]. Materials Science & Engineering A, 1993, 163(1): 115−125.

[19] DUTTA I, HARPER C P, DUTTA G. Role of Al_2O_3 particulate reinforcements on precipitation in 2014 Al-matrix composites[J]. Metallurgical & Materials Transactions A, 1994, 25(8): 1591−1602.

[20] BRONSVELD P M, STARINK M J, VERWERFT M, DE HOSSON J TH M, VAN MOURIK P. Observations of precipitation in a particle-reinforced Al-Cu-Mg alloy with 20% silicon[J]. Scripta Metallurgica Et Materialia, 1995, 33(3): 427−432.

[21] WOLVERTON C. Crystal structure and stability of complex precipitate phases in Al-Cu-Mg-(Si) and Al-Zn-Mg alloys[J]. Acta Materialia, 2001, 49(16): 3129−3142.

[22] RAVI C, WOLVERTON C. First-principles study of crystal structure and stability of Al-Mg-Si-(Cu) precipitates[J]. Acta Materialia, 2004, 52(14): 4213−4227.

[23] KIM K, BOBEL A, BRAJUSKOVIC V, ZHOU B C, WALKER M, OLSON G B, WOLVERTON C. Energetics of

native defects, solute partitioning, and interfacial energy of Q precipitate in Al-Cu-Mg-Si alloys[J]. Acta Materialia, 2018, 154: 207−219.

[24] OUYANG Y F, LIU F L, LU T, TAO X M, DU Y, HE Y H. First-principles investigation of the mechanical, electronic and thermophysical properties of *Q*-phase in Al-Mg-Si-Cu alloys[J]. Computational Materials Science, 2013, 67: 334−340.

[25] ZHANG F, DU Y, LIU S H, JIE W Q. Modeling of the viscosity in the AL-Cu-Mg-Si system: Database construction[J]. Calphad, 2015, 49: 79−86.

[26] CUI S, JUNG I H. Thermodynamic modeling of the quaternary Al-Cu-Mg-Si system[J]. Calphad, 2017, 57: 1−27.

[27] LÖFFLER A, ZENDEGANI A, GRÖBNER J, HAMPL M, SCHMID-FETZER R, ENGELHARDT H, RETTENMAYR M, KÖRMANN M, HICKELT, NEUGEBAUER J. Quaternary Al-Cu-Mg-Si *Q* phase: Sample preparation, heat capacity measurement and first-principles calculations[J]. Journal of Phase Equilibria and Diffusion, 2016, 37(2): 119−126.

[28] CHANG K, LIU S, ZHAO D, DU Y, ZHOU L, CHEN L. Thermodynamic description of the Al-Cu-Mg-Mn-Si quinary system and its application to solidification simulation[J]. Thermochimica Acta, 2011, 512(1/2): 258−267.

[29] TSAI M H, YEH J W. High-entropy alloys: A critical review[J]. Materials Research Letters, 2014, 2(3): 107−123.

[30] MIRACLE D B, SENKOV O N. A critical review of high entropy alloys and related concepts[J]. Acta Materialia, 2017, 122: 448−511.

[31] VAIDYA M, MURALIKRISHNA G M, MURTY B S. High-entropy alloys by mechanical alloying: A review[J]. Journal of Materials Research, 2019, 34(5): 664−686.

[32] ZHANG Y, ZHOU Y J, LIN J P, CHEN G L, LIAW P K. Solid-solution phase formation rules for multi-component alloys[J]. Advanced Engineering Materials, 2008, 10(6): 534−538.

[33] YANG X, ZHANG Y. Prediction of high-entropy stabilized solid-solution in multi-component alloys[J]. Materials Chemistry and Physics, 2012, 132(2/3): 233−238.

[34] ZHANG Y, ZUO T T, TANG Z, GAO M C, DAHMEN K A, LIAW P K, LU Z P. Microstructures and properties of high-entropy alloys[J]. Progress in Materials Science, 2014, 61: 1−93.

[35] ZHANG R F, LIU B X. Proposed model for calculating the standard formation enthalpy of binary transition-metal systems[J]. Applied physics letters, 2002, 81(7): 1219−1221.

[36] ZHANG R F, SHENG S H, LIU B X. Predicting the formation enthalpies of binary intermetallic compounds[J]. Chemical Physics Letters, 2007, 442(4/6): 511−514.

[37] SUN S P, YI D Q, JIANG Y, ZANG B, XU C H, LI Y. An improved atomic size factor used in Miedema's model for binary transition metal systems[J]. Chemical Physics Letters, 2011, 513(1/3): 149−153.

[38] CHOU K C. A general solution model for predicting ternary thermodynamic properties[J]. Calphad, 1995, 19(3): 315−325.

[39] OUYANG Y F, ZHONG X P, DU Y, FENG Y P, HE Y H. Enthalpies of formation for the Al-Cu-Ni-Zr quaternary alloys calculated via a combined approach of geometric model and Miedema theory[J]. Journal of Alloys and Compounds, 2006, 420(1/2): 175−181.

[40] 张 雷, 王戎丞, 陶小马, 欧阳义芳. Al-Cu-RE 三元合金热力学性质的 Miedema 理论计算[J]. 稀有金属材料与工程, 2015, 44(3): 628−633.
ZHANG Lei, WANG Rong-cheng, TAO Xiao-ma, OUYANG Yi-fang. Thermodynamic properties of Al-Cu-RE ternary alloys calculated with Miedema's theory[J]. Rare Metal Materials and Engineering, 2015, 44(3): 628−633.

[41] ZHANG L, CHEN H M, OUYANG Y F, DU Y. Amorphous forming ranges of Al-Fe-Nd-Zr system predicted by Miedema and geometrical models[J]. Journal of Rare Earths, 2014, 32(4): 343−351.

[42] ŚNIADECKI Z, NAROJCZYK J W, IDZIKOWSKI B. Calculation of glass forming ranges in the ternary Y-Cu-Al system and its sub-binaries based on geometric and Miedema's models[J]. Intermetallics, 2012, 26: 72−77.

[43] DE BOER F R, MATTENS W C M, BOOM R, MIEDEMA A R, NIESSEN A K. Cohesion in metals[M]. Amsterdam: North-Holland Press, 1988.

[44] KITTEL C. Introduction to solid state physics[M]. New York: John Wiley & Sons Press, 2005.

[45] PHRAGMÉN G.. On the phases occurring in alloys of aluminium with copper, magnesium, manganese, iron, and silicon[J]. Journal of the Institute of Metals, 1950, 77(6): 489−551.

[46] CAYRON C, BUFFAT P A, BEFFORT O, LONG S. Effect of SiO_2 binder on the precipitation state of an $AlCu_4Mg_1Ag$/Saffil composite[J]. Journal of Materials Science, 1999, 34(5): 905−915.

[47] MONDOLFO L F. Aluminum alloys: Structure and

properties[M]. London: Butterworths Press, 1979.

[48] ARNBERG L, AURIVILLIUS B. The crystal structure of $Al_xCu_2Mg_{12-x}Si_7$, (h-AlCuMgSi)[J]. Acta Chemica Scandinavica, 1980, 34(A): 1−5.

[49] MIEDEMA A R, DE CHATEL P F, DE BOER F R. Cohesion in alloys-fundamentals of a semi-empirical model[J]. Physica B+C, 1980, 100(1): 1−28.

[50] TAKEUCHI A, INOUE A. Calculations of mixing enthalpy and mismatch entropy for ternary amorphous alloys[J]. Materials Transactions, JIM, 2000, 41(11): 1372−1378.

Thermodynamics study of Al-based high entropy quinary alloys

ZHANG Lei[1, 3], CHEN Hong-mei[2], TAO Xiao-ma[2], OUYANG Yi-fang[2]

(1. School of Mathematics and Information Science, Guangxi College of Education, Nanning 530023, China;
2. College of Physical Science and Technology, Guangxi University, Nanning 530004, China;
3. Institute for Intelligent computing and simulation Research, Guangxi College of Education, Nanning 530023, China)

Abstract: High entropy alloys (HEAs) have attracted attentions due to their high hardness, high strength, good wear resistance and corrosion resistance. HEAs generally have at least five principle elements, and the entropy of mixing can be increased by the addition of elements. The solid-solution phase is formed in HEAs with a simple lattice structure. The mixing enthalpies for multi-component alloys can be calculated by Miedema's theory and geometrical model, and the mixing enthalpy is important for the solid-solution forming. The mixing enthalpies of solid-solution for $Al_x(CuMgSi\text{-}T)_{1-x}$ (T=Ag, As, Au, B, Ba, Be, Bi, C, Ca, Cd, Co, Cr, Cs, Fe, Ga, Ge, Hf, Hg, In, Ir, K, La, Li, Mn, Mo, N, Na, Nb, Ni, Os, P, Pb, Pd, Pt, Rb, Re, Rh, Ru, Sb, Sc, Sn, Sr, Ta, Tc, Ti, Tl, V, W, Y, Zn, Zr) quinary alloys have been calculated by Miedema's theory and the extend geometric model, and the forming composition ranges of $Al_x(CuMgSi\text{-}T)_{1-x}$ system have been predicted according to the criteria of the mixing entropy and the atomic size differences. The calculated enthalpy of mixing indicates that some compositions for $Al_x(CuMgSi\text{-}T)_{1-x}$ systems are easy to form HEAs. The method of predicting the composition forming ranges for HEAs by the criteria of the mixing enthalpy and parameter δ is simple, the predicted mixing enthalpies could be benefit to the investigations of composition design for HEAs.

Key words: Miedema's theory; geometrical model; high entropy alloy; mixing enthalpy; atomic size; square deviation

Foundation item: Projects(51531009, 11464001) supported by the National Natural Science Foundation of China; Project(2016GXNSFBA380166) supported by the Natural Science Foundation of Guangxi Province, China; Project(2017KY1472) supported by the Science Foundation of Guangxi Education Department, China

Received date: 2018-12-02; **Accepted date:** 2019-04-02

Corresponding author: OUYANG Yi-fang; Tel: +86-771-3237386; E-mail: ouyangyf@gxu.edu.cn

(编辑　何学锋)